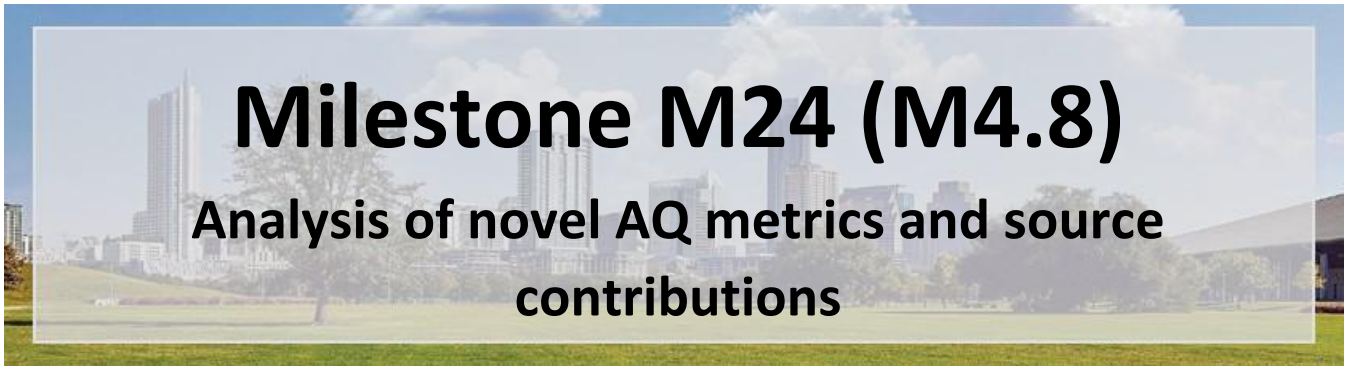

Milestone M24 (M4.8)

Analysis of novel AQ metrics and source contributions

RI-URBANS

Research Infrastructures Services Reinforcing Air Quality Monitoring Capacities in European Urban & Industrial AreaS (GA n. 101036245)

By

PSI, CSIC, NOA & CNRS

19/09/2024

RI-URBANS (www.RIURBANS.eu) is supported by the European Commission under the Horizon 2020 – Research and Innovation Framework Programme, H2020-GD-2020, Grant Agreement number: 101036245

Milestone M24 (M4.8): Analysis of novel AQ metrics and source contributions

Authors: Kaspar Rudolf Daellenbach (PSI), Andrés Alastuey (CSIC), Nikos Mihalopoulos (NOA), Gaëlle Uzu (CNRS), Barend L. van Drooge (CSIC), Marjan Savadkoohi (CSIC), Meritxell Garcia-Marlès (CSIC), Jean Luc Jaffrezo (UGA)

Work package (WP)	WP4 / Pilot implementations for testing and demonstrating services
Milestone	M24 (M4.8)
Lead beneficiary	PSI
Means of verification	Analysis completed
Estimated delivery deadline	M36 (30/09/2024)
Actual delivery deadline	19/09/2024
Version	Final
Reviewed by	WP4 leaders
Accepted by	Project Coordination Team
Comments	This is a document describing the analysis performed in Pilot 4 on Novel Health Indicators of nanoparticles and PM components and source contributions.

RI-URBANS (www.RIURBANS.eu) is supported by the European Commission under the Horizon 2020 – Research and Innovation Framework Programme, H2020-GD-2020, Grant Agreement number: 101036245

Table of Contents

RI-URBANS (www.RIURBANS.eu) is supported by the European Commission under the Horizon 2020 – Research and Innovation Framework Programme, H2020-GD-2020, Grant Agreement number: 101036245

1 About this document

This report offers a summary of the analysis of novel air quality (AQ) metrics and source contributions at selected urban background locations in Europe. This includes emerging AQ metrics such as off-line particulate matter (PM) chemistry, equivalent Black Carbon (eBC), Particle Number Size Distribution (PNSD), as well as PM's oxidative potential (OP). Based on the presented work, main conclusions on source contributions in urban environments in Europe are drawn. The underlying data is available to the RI-URBANS partners at https://www.healthpilot-riurbans.eu.

This is a public document that will be distributed to all RI-URBANS partners for their use and submitted to European Commission as a RI-URBANS Milestone M24 (M4.8). This document can be downloaded at https://riurbans.eu/work-package-4/#milestones-wp4

2 Methods

In RI-URBANS, Pilot cities were selected based such that 1) geographical variation in Europe is covered, and 2) large populations to facilitate potential use of the generated data in epidemiological assessments. Initially, Athens (Greece), Barcelona (Spain), and Zurich (Switzerland) were selected. Later on, Paris (France) - as one of the major metropolitan areas - was incorporated (see 2.1) even though not part of this milestone. Measurement of novel metrics, including eBC, PNSD, PM composition and OP were performed following the recommendations of D1 (D1.1) generated within the framework of RI-URBANS WP1 and providing guidelines to measure the selected non-regulated pollutants and perform quality analysis.

2.1 Sampling sites

Within this milestone, scientific work was carried out at four geographical locations (Figure 1): Athens Thissio (Greece), Barcelona Palau Reial (Spain), Paris Les Halles (France), and Zurich Kaserne (Switzerland).

Athens Thissio

The Athens Thissio Air Monitoring Station is located on the top of the hill of Nymphs at the National Observatory of Athens (37.97°N, 23.72° E) around 50 m above the mean city level. It is an urban background station close to the city centre, which receives aerosols both from urban and regional sources. Surrounding the area is a pedestrian zone, while there is no major road within a 500 m radius from the station.

Barcelona Palau Reial

The Barcelona Palau Reial urban background monitoring site is located within the grounds of the IDAEA - CSIC in northwest Barcelona, *(41° 23'14.28"N, 2°6'56.34"E, 77* m a.s.l*),* located 200 m from one of the main traffic avenues of the city (Diagonal Avenue, traffic density of 90 000 vehicles per working day). The main source of atmospheric PM is road traffic, although contributions from industry, regional secondary atmospheric pollutants, construction, and shipping are also relevant. Atmospheric dynamics are driven by the breeze circulation regime, with a NW wind component during the night and the development of breezes during the day turning progressively from SE to SW direction, with gradually increasing wind speeds reaching maximum values around noon. This supersite is a National Facility (NF) for in situ measurements in ACTRIS - ERIC, and forms part of the Catalan Air Quality Monitoring Network (AQMN). It is a well-equipped infrastructure for in-situ characterization of aerosols (optical, physical, and chemical offline and online) and trace gases (NO_x, SO_2, O_3, CO).

RI-URBANS (www.RIURBANS.eu) is supported by the European Commission under the Horizon 2020 – Research and Innovation Framework Programme, H2020-GD-2020, Grant Agreement number: 101036245

Paris Les Halles

The urban background station at Paris-Les Halles is located in the city centre of Paris. The station is in a public park (Jardins des Halles) adjacent to the infrastructure of the local public transportation network Châtelet Les Halles (48° 51' 43.74" N, 2° 20' 40.71"*W*). The surrounding area is a typical urban neighbourhood with residential and commercial activities.

Zurich Kaserne

The Zurich Kaserne urban background monitoring site is located in a courtyard park in the city centre of Zurich (47° 22′ 42′′ N, 8° 31 ′52′′ E, 410 m a.s.l.), part of the Swiss National Monitoring Network (NABEL). The surrounding area is dominated by residential buildings and small businesses. While the station is not directly affected by major roads, local traffic is present. The station receives aerosols both from regional and local/urban sources.

***Figure 1**. Pilot 4 Monitoring sites: Athens, Barcelona, Paris and Zurich.*

RI-URBANS (www.RIURBANS.eu) is supported by the European Commission under the Horizon 2020 – Research and Innovation Framework Programme, H2020-GD-2020, Grant Agreement number: 101036245

2.2 Online measurement of novel metrics

2.2.1 Measurement of eBC

At all sites, eBC concentrations are measured and calculated by filter absorption photometers (FAPs) from Aethalometers (AE33) software through two steps. In the first step (Step 1) the measured attenuation (ATN) is converted into absorption coefficient (ABS). For this, two artifacts related to the presence of the filter tape are considered. One artifact consists in an increase of the measured ATN due to the scattering of light by the filter tape (C_0). The other artifact consists in the progressive loss of sensitivity due to the progressive accumulation of particles on the filter tape (factor loading effect; FL). In the second step (Step 2) the ABS is converted into eBC mass concentrations assuming a specific and constant mass absorption cross section (MAC) of BC particles.

Step 1: All AE instruments convert ATN to ABS using predefined and constant C_0 that depends on the filter tape used. For the new filter tape (M8060) C_0 is 1.39. The filter tape M8060 is the recommended one (available since October 2017). The C_0 values are set in the instrument software and must be changed manually if the filter tape is replaced with a different one (Savadkoohi et al., 2023). The new AE33 model corrects online for FL by applying the "dual spot" method (Drinovec et al., 2015).

Step 2: The AE33 model calculates eBC from ATN at 880 nm using a MAC of 7.77 m^2g^{-1} at 880 nm and C_0=1.39 depending on the filter tape used.

eBC source apportionment is commonly performed using the Aethalometer (AE) approach (Sandradewi et al., 2008). AE approach uses the seven absorption coefficient measurements provided by AE instruments. ACTRIS provides the harmonization factors necessary to convert the ATN measured with AE instruments into ABS. These harmonization factors are needed because the C_0 is different from the one used in the AE software (see Savadkoohi et al., 2023, 2024, and ST2 on BC from RI-URBANS for more details).

2.2.2 Measurement of ultrafine particles (UFP)

Measurements of Particle Number Concentration (PNC) and Particle Number Size Distribution (PNSD) of UFP are conducted at all sites by using Condensation Particle Counters (CPCs) and Mobility particle size spectrometers (MPSSs), respectively, in accordance with ACTRIS and CEN guidelines and (ACTRIS, 2021; CEN/–S16976:2016; CEN/TS17434:2020), and ST1 on UFP-PNSD from RI-URBANS. These guidelines recommend a size measurement range of 10-800 nm and allow the measurement of particles with diameters below 10 nm if required. Data harmonisation is performed according to the methods described by (Trechera et al., 2023) and (Garcia-Marlès et al., 2024a). The data is averaged hourly, and the measurement range is limited to 10-800 nm to ensure better comparability between the sites.

RI-URBANS (www.RIURBANS.eu) is supported by the European Commission under the Horizon 2020 – Research and Innovation Framework Programme, H2020-GD-2020, Grant Agreement number: 101036245

2.3 PM composition and OP

2.3.1 Sampling and analytical strategies

Given the different chemical composition and sources of fine PM and coarse PM, at each pilot city, PM2.5 and PM10 were sampled simultaneously for 1 year – 1 full seasonal cycle for subsequent chemical offline analyses. Given constraints defined by the elaborate chemical characterization, not every day of the year was characterized but instead every 2nd day (Barcelona, Athens, Paris). Zurich was used as a frontrunner (sampled every 4th day) based on which, the analytical strategy was defined, e.g. increased sampling frequency. This is more than for Zurich (every 4th) to allow for a better data coverage, while keeping the analytical load under control.

To obtain enough PM sample to perform all the analyses planned, PM sampling was performed by using high-volume samplers (HiVol, 30 m^3 h^{-1}; DH80 DIGITEL, Switzerland/Austria; and CAVA/MSb - MCV, Spain), equipped with PM10 and PM2.5 heads. The samples were collected on 15-cm diameter ultrapure quartz microfiber filters (Pall). Sampling period and number of samples collected at each site are shown in Table 1.

The PM mass on the filter were determined using the En12341:2014 (PM10) and En14907:2005 (PM2.5) gravimetrical procedures at each sampling location by the collecting institution. In short, gravimetric concentration of PM was obtained by weighing the filter samples before and after sampling, after 48 h stabilization at 20 °C and 50 % RH.

A complete chemical characterization was performed based on the PM2.5 and PM10 Quartz filters (Pall). For optimal comparability of the results, each type of analysis was performed centrally in 1 lab, except for specific analysis in Paris that decided to join the activities later (and is not part of the deliverable). In these cases, an intercomparison with Pilot central labs was carried out. After gravimetric analysis, punches of filters were distributed to each laboratory for centralized analysis (Figure 2). Table 2 summarizes the analyses performed and the laboratory responsible for each analytical task.

Blank filters from the same filter box underwent the same sample treatment and measurements, and its values were subtracted from the corresponding samples.

***Table 1**. Sampling period and number of samples collected and analysed at each site are shown*

Site	Period	PM10 samples	PM2.5 samples
Zurich Kaserne	06/2018-05/2019	91	91
Barcelona Palau Reial	03/2022-02/2023	175	160
Athens Thissio	03/2022-02/2023	159	155
Paris Châtelet-Les Halles	04/2022-03/2023	124	169

RI-URBANS (www.RIURBANS.eu) is supported by the European Commission under the Horizon 2020 – Research and Innovation Framework Programme, H2020-GD-2020, Grant Agreement number: 101036245

***Table 2**. Laboratory and method for each PM component analysed.*

PM component	Responsible Laboratory	Method
Metals: **total concentration** **soluble fraction**	 CSIC NOA	 ICP-OES ICP MS ICP MS
Water soluble ions	NOA Paris (UGA)	IC IC-MS
OC/EC	CSIC Paris:INERIS(PM_{10}), AirParif ($PM_{2.5}$)	Thermo-optical analyser (SUNSET)
Brown carbon	NOA	UV–Vis spectrophotometry
Organic tracers: PAHs, Acids**,** Sugars and polyols	CSIC Paris: UGA	GC-MS LC-MSMS. Includes tetrols
WSOC	PSI	Shimadzu TOC analyzer
Non-targeted mass spectral WSOA characterization	PSI	Aerosol Mass Spectrometer, extractive electrospray ionization mass spectrometer
Brown Carbon (BrC) at all 4 sites	NOA	BrC measurements in water- and methanol- extracts were performed by UV–Vis spectrophotometry
Oxidative potential	UGA	acellular AA and DTT assays

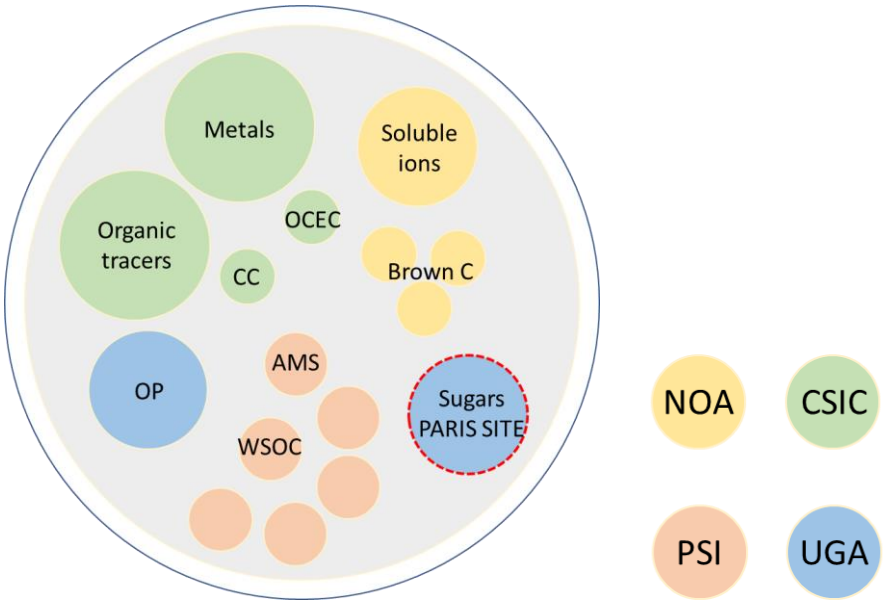

***Figure 2.** Distribution of punches for analytical.*

RI-URBANS (www.RIURBANS.eu) is supported by the European Commission under the Horizon 2020 – Research and Innovation Framework Programme, H2020-GD-2020, Grant Agreement number: 101036245

The offline chemical analyses performed at the pilot locations include the components put forward in the new EU AQ Directive (NAQD, CEU, 2024) but go further in detail to explore the added value of specific source tracers. In the following the protocols applied for performing the different chemical analyses are described in detail.

2.3.2 Total concentration of metals

Determination of concentration of major elements and metals was carried out at the IDAEA-CSIC laboratories following the methodology proposed by (Querol et al., 2001).This method requires a complete previous dissolution of the samples. Samples are bulk acidic dissolved using HNO_3:HF:$HClO_4$, which has been widely used. This procedure allows the complete digestion of silicon-containing compounds, and other specific minerals (e.g. TiO_2). This is necessary for source apportionment analyses where road dust, non-exhaust vehicle PM, demolition/construction dust or desert dust is intended to be included, this type of digestion is required. Acidic digestion and analysis of all samples collected at all sites (including Zurich) was performed at the IDAEA-CSIC Laboratories.

One punch of 45 mm diameter of each sample underwent acid digestion pre-treatment (HNO_3:HF:$HClO_4$), and the resulting acidic solutions were subsequently analysed using Inductively Coupled Plasma Atomic Emission Spectrometry (ICP-AES, ICAP 6500 Radial View, Thermo Fisher Scientific, US) to determine the concentration of major elements (Al, Ca, Cu, Fe, K, Mg, Mn, Na, P, and S) and Inductively Coupled Plasma Mass Spectrometry (ICP-MS, iCAP-RQ, Thermo fisher Scientific, US) to measure the concentration of trace elements (Li, Be, Sc, Ti, V, Cr, Mn, Co, Ni, Cu, Zn, Ga, Ge, As, Se, Rb, Sr, Y, Zr, Nb, Mo, Cd, Sn, Sb, Cs, Ba, La, Ce, Pr, Nd, Sm, Eu, Gd, Tv, Dy, Ho, Er, Tm, Yb, Lu, Hf, Ta, W, TI, Pb, Bi, Th, and U- The accuracy of the ICP-AES and ICP-MS analyses was investigated by analysing 3–10 mg of the National Institute for Standards and Technology-1633b (fly ash) reference material loaded on a 150-mm blank filter (Amato et al., 2009). See ST3 on PM speciation from RI-URBANS.

2.3.3 Water soluble ions

Analysis of water-soluble ions followed the standard (En16913:2017). Water extraction was performed at NOA labs for samples collected at Athens and Barcelona. The same constituents for Paris and Zurich were analysed by UGA. At first, a piece with 1.5 cm^2 surface area was obtained from each filter that collected atmospheric samples using appropriate tools. The pieces were then placed inside dry plastic bottles and extracted with 10mL of ultrapure water. Then, they were placed inside an ultrasound system for 45 minutes to aid dilution. After the extraction, the bottles were left to cool down and a few chloroform ($CHCl_3$) drops were added in order to prevent bacterial deterioration and preserve the concentrations while the samples were stored in the fridge until analysis. The major aerosol cations (Ca^{2+}, Mg^{2+}, Na^+, K^+, NH_4^+) and anions (SO_4^{2-}, NO_3^-, Cl^-) were analyzed by Ion Chromatography (IC; Dionex-500; Thermo Fischer Scientific) following the methodology described in (Paraskevopoulou et al., 2015). All analytical results were blank-corrected. For the anions the mobile phase used was a mixture of sodium bicarbonate and sodium carbonate $NaHCO_3$ / NaH_2CO_3 with an isocratic elution flow rate of 1.5 mL/min. For the cations (NH_4^+, Na^+, K^+, Mg^{2+}, Ca^{2+}) the mobile phase used is methanesulfonic acid (MSA), a strong acid that dissociates and releases H^+ which substitute the cations inside the column. Isocratic elution with a flow rate of 1 mL/min was selected. Before analyzing the extracted samples, each sample was filtrated using a CHROMAFIL 0.15 µm with 0.45 µm pore size filter and then transferred inside smaller glass vials that were placed on the autosampler. This way particles or impurities that could damage the chromatography system were removed. See ST3 on PM speciation from RI-URBANS.

2.3.4 Water soluble concentration of metals

The water extraction solution (2.3.3) was used for the analysis of water soluble metals by using an ICP-MS. Especially water soluble Trace elements (Al, Ca, Mn, Fe, V, Cr, Ni, Cu, Zn, Cd, As and Pb) were determined by Inductively Coupled Plasma Mass Spectrometry (ICP-MS, Perkin Elmer, NexION 300X) following the procedure described in

RI-URBANS (www.RIURBANS.eu) is supported by the European Commission under the Horizon 2020 – Research and Innovation Framework Programme, H2020-GD-2020, Grant Agreement number: 101036245

Theodosi et al. (2018). Yttrium (Y) and Indium (In) were added as internal standards, and all reported concentrations were corrected for blanks. This analysis was performed at NOA for Barcelona, Zurich, Paris and Athens samples.

2.3.5 Organic and elemental carbon

To determine the concentration of OC and EC, collected in quartz fibre filters, we follow the En16909:2017 , for the measurement of airborne EC and OC in PM2.5 (Karanasiou et al., 2015; Brown et al., 2017). (En16909:2017) adopted the EUSAAR2 thermal protocol (Cavalli et al., 2010) as the reference methodology for the determination of EC and OC in ambient PM2.5. All filters (except those collected at Paris Les Halles) were analysed at the IDAEA-CSIC laboratory by using a Sunset. IDAEA CSIC participates in the intercomparison exercises organised by CAIS-ECAC. See ST3 on PM speciation from RI-URBANS.

2.3.6 Brown carbon

Brown carbon (BrC) measurements in water- and methanol- extracts were performed by UV–Vis spectrophotometry (Hecobian et al., 2010; Srinivas et al., 2016). A 1 cm2 punch was placed in 15 mL of ultrapure water and another in 15 mL of methanol. The water-soluble fraction was extracted by ultrasonication for 30 min (Paraskevopoulou et al., 2023). For methanol extraction, punches remained in the solvent for 24 h at room temperature (Shetty et al., 2019; Atwi et al., 2022). For more details please refer to (Paraskevopoulou et al., 2023).

2.3.7 Organic tracers

The analysis of molecular organic compounds involved solvent extraction followed by gas chromatography-mass spectrometry (GC-MS), enabling the detection and quantification of a wide range of organic compounds with varying polarities. Up to seventy-two compounds were detected in ambient air and emission sources, many of which serve as molecular tracers of sources and atmospheric processes (Alier et al., 2013). Modifications of the extraction method described by (Fontal et al., 2015) were implemented and described by (Van Drooge et al., 2023)

A filter punch (3.4 mm diameter) was taken from whole filter samples and 25 µL of deuterated PAH standard (50 ppb) in cyclo-hexane was added to a conic vial. Another punch sample for acids and sugars analysis, was extracted in 25 µL methanol containing deuterated succinic acid-D4 and levoglucosan-D7 (3 ppm). Extraction took place in ultrasonic bath for 15 minutes. Then, the filter punch was removed and the PAHs extract was injected into GC-MS. Acid and sugar extracts were evaporated to dryness under gentle nitrogen gas stream and 25 µL bis(trimethylsilyl)trifluoroacetamide (BSFTA)+ 1% TMCS and 10 µL pyridine was added to vial to facilitate the formation of trimethylsilyl (TMS) derivatives of polar compounds for 30 minutes at 70ºC in oven before injection into GC-MS. Instrumental analysis was conducted using a GC-MS (Agilent 7890 GC with 5975 MSD), operating in full scan mode with electron impact ionization for polar compounds and in SIM mode for PAHs. Compound quantification utilized an internal standard method and corrections were made for procedural losses using surrogate standards. Field and analytical blanks were performed during sample analysis. Identified organics were confirmed by retention time, characteristic mass fragments, and comparison with spectral libraries. Organic compounds were analysed and identified based on their mass spectra and retention times. See ST3 on PM speciation from RI-URBANS.

2.3.8 Non-targeted chemical characterization of water-soluble OA

As explorative addition, the water-soluble organic PM fraction was characterized based on aqueous extractions of a filter portion in milliQ water, following the protocols presented in (Daellenbach et al., 2016; Daellenbach et al., 2020; Cui et al., 2024). In a first step, the bulk quantities water-soluble organic carbon and water-soluble inorganic carbon were quantified with a Shimadzu TOC analyzer. In a next step, the same extracts were used for non-targeted chemical characterisations. For Zurich, such analyses were performed using an Aerosol Mass Spectrometer following the approaches presented in (Cui et al., 2024). The results showed a good chemical resolution while still

RI-URBANS (www.RIURBANS.eu) is supported by the European Commission under the Horizon 2020 – Research and Innovation Framework Programme, H2020-GD-2020, Grant Agreement number: 101036245

limited by the hard ionization in the mass spectrometer leading to excessive fragmentation of the analyses. This resulted in a loss of chemical information. For that reason, we used a soft-ionization mass spectrometer (Extractive Electrospray Ionization Mass Spectrometer: EESI-MS) for Athens, Barcelona, and Paris following (Cui et al., 2024).

2.3.9 Oxidative potential

PM's oxidative potential was measured with two assays: Ascorbic Acid (AA) and dithiothreitol (DTT). The PM collected on quartz fiber filters was extracted in simulated lung fluid (no filtration step to keep the insoluble parts) at iso-concentrations of 25 µg/ml. The protocols followed (Calas et al., 2018; Calas et al., 2019; Calas et al., 2017). See ST4 on OP of PM from RI-URBANS.

2.3.10 Mass closure / data treatment

PM components determined have been grouped into: organic matter (OM) derived from OC, elemental carbon (EC), secondary inorganic aerosols (SIA) including SO_4^{2-}, NO_3^- and NH_4^+, mineral dust and sea-salt.

The methodology for estimating the sea-salt and mineral dust fraction is the one proposed by Alastuey et al. (2016). Some elements such as Na, Mg, Ca and K are associated with both mineral dust and sea-salt aerosol. The sea-salt contribution was estimated for each element before estimating the mineral load. The concentrations of these elements in seawater are well known and therefore it is possible to estimate the marine contribution to PM mass once we know the concentration of one of these elements. Due to the potential volatilization of Cl by the interaction between NaCl with acidic species, the sea salt fraction of each species was estimated based on the concentration of marine Na. Thus, given that Na can be partially related to mineral dust, first, we calculated the mineral fraction of Na from the content of Al by using the ratio determined by (Moreno et al., 2006) for soils and dust in North Africa. Thus, the mineral sodium (non-sea-salt sodium, Na_{dust}) was obtained by multiplying Al concentration by 0.12, and the sea-salt fraction of Na (Na_{ss}) can be estimated by subtracting Na_{dust} from the total Na. The sea-salt fraction of calcium, magnesium, potassium and sulphate was estimated by using their seawater ratios concerning Na_{ss} (Nozaki, 1997). Finally, the total sea-salt load was determined by the sum of Cl^-, Na_{ss}, Ca_{ss}, Mg_{ss}, K_{ss} and $SO_4^{2-}{}_{ss}$. The non-sea-salt (nss) fractions of Ca, Mg, Mn, Na, K and SO_4^{2-} were obtained by subtracting the previously calculated sea-salt fraction from their bulk concentration. In addition to the sea salt fraction, K can be related to mineral (K_{dust}) and biomass burning (K_{bb}). The mineral fraction is estimated from Al ($K_{dust} = 0.31 \cdot Al$, (Moreno et al., 2006), and the biomass fraction by the difference: $K_{bb} = K - K_{ss} - K_{dust}$. Finally, the total mineral dust concentration was determined by addition of the concentrations of all mineral related elements expressed as oxides, such as Al_2O_3, SiO_2, Fe_2O_3, TiO_2, P_2O_5, CaO_{dust}, MgO_{dust}, Na_2O_{dust}, and K_2O_{dust}. Assuming the major presence of CaO_{dust} as CaCO3, the $CaCO_3$ was estimated from CaO_{dust} by multiplying by 1.274. This methodology can be only applied when the bulk concentrations of major elements (Al, Si, Ca, Mg, Fe, Na, K) is determined. Since the elemental concentration was determined from acidic digestion by ICP methods Si was not determined and we estimated it from Al content by multiplying Al content by 3 (Alastuey et al., 2016). Organic matter (OM) or organic aerosol (OA) has been estimated from organic carbon (OC), applying an OM:OC factor of 1.8.

RI-URBANS (www.RIURBANS.eu) is supported by the European Commission under the Horizon 2020 – Research and Innovation Framework Programme, H2020-GD-2020, Grant Agreement number: 101036245

2.4 Source apportionment analysis

2.4.1 Particulate Matter chemistry

Positive Matrix Factorization (PMF, (Paatero and Tapper, 1994) is the most common receptor model used for source apportionment and it is based on the mass conservation principle:

$$x_{ij} = \sum_{k=1}^{p} g_{ik} f_{jk} + e_{ij} \quad i = 1, 2, \cdots, m \quad j = 1, 2 \cdots n$$

where x_{ij} is the concentration of the species j in the i^{th} sample, g_{ik} is the concentration of the k^{th} source in the i^{th} sample, f_{jk} is the contribution of the species j in source k and e_{ij} is the residual concentration. PMF can be solved with the Multilinear Engine (ME-2) developed by (Paatero, 1999) and implemented in the US EPA PMF v5. In this study, the US EPA PMF v5 (Norris et al., 2014) was applied to the three datasets independently. A harmonization method is applied to each dataset, including input chemical species, uncertainty calculation, result validation criteria, and implementation steps to ensure the homogeneity of PM source apportionment results. Input chemical species are chosen based on the well-known source tracers, as presented in various studies (Weber et al., 2019; Waked et al., 2014). In addition, organic species are added to identify sources of organic aerosols and elucidate the fate of these organics in the atmosphere (Borlaza et al., 2021; Glojek et al., 2024). The measurement uncertainty is important in the PMF model as its algorithm is based on the weighted least squares method, where uncertainty is considered as the weighting. Uncertainty is calculated using concentration and analysis error (Gianini et al., 2013), denoting that a species with higher uncertainty has less influence in the PMF model. See ST10 on PM source apportionment from RI-URBANS.

Criteria for validation were chosen based on European recommendations for using the receptor model (Mircea et al., 2020). These are: (1) low influence of data outliers based on the ratio of $Q_{true}/Q_{robust} < 1.5$. (2) The presence of trace species in the profile and the temporal evolution are clear enough to identify a source. (3) All factors should have a contribution > 1% to the total variable PM10. (4) The distribution of residuals from -3 to 3 indicates the absence of outliers and the feasibility of reconstruction. (5) The correlation coefficient between species concentration measured and predicted by PMF must be greater than 0.5. (6) Good bootstrap value: represents the stability of the solution: at least, 70 runs per 100 runs, where the correlation between the base run and boot runs is greater than 0.6. For each data set, the PMF is run from 4 to 12 factors to observe the evolution of the chemical profile and contribution over the number of factors. For each run, the solution is attentively evaluated using the validation criteria. The results of the different inputs/number of factors are compared to determine the most appropriate solution.

2.4.2 Particle Number Size Distribution of ultrafine particles

Source apportionment of PNSD was performed following the methodology proposed by (Garcia-Marlès et al., 2024b) relying on PMF - the same receptor model as for the source apportionment using the PM chemistry (section 2.4.1). Given the large datasets that cannot be handled by US EPA PMF, source apportionment was performed using the tool developed by (Hopke et al., 2023) using ME-2. The datasets included hourly averaged PNSD data combined with hourly concentrations of the ancillary co-pollutants (eBC, PM_X, NO_2, NO, SO_2, O_3 and CO, when available), to help the identification of the sources. PMF requires individual uncertainty estimates for each data value. Detailed information about the estimation of uncertainties in the PNC and PNSD values will be published in Garcia-Marlès et al. (2024b). See ST11 on UFP-PNSD source apportionment from RI-URBANS.

The datasets for each site were independently analysed by PMF. PMF was run multiple times for different numbers of factors (sources). Factor profiles and contributions that were obtained were plotted to explore their physical interpretability. If the results were not consistent, PMF was run again with a different number of factors. Then, the number of sources was finally determined, examining the results and choosing the best solution. The solutions were

RI-URBANS (www.RIURBANS.eu) is supported by the European Commission under the Horizon 2020 – Research and Innovation Framework Programme, H2020-GD-2020, Grant Agreement number: 101036245

selected according to the accepted criteria and guidelines (Hopke et al., 2023; Belis et al., 2019), considering: (i) scaled residuals approximately randomly distributed between -3 and 3, (ii) a Qtrue/Qexp ratio close to 1, (iii) profile uncertainties determined by the displacement (DISP) method, and (iv) the provision of the most physically meaningful profiles and temporal behaviours. To support the identification of the sources, the contributions of each factor to the variance of the co-located ancillary pollutants, daily patterns, seasonality, and polar plots were evaluated, and sources were identified using existing literature. The data analysis and plots were performed with the R statistical software (v4.2.3) and the package *Openair* (Carslaw and Ropkins, 2012). Source apportionment results from this study (from 2020-2023) will be compared to those obtained by (Garcia-Marlès et al., 2024b) for the period 2009-2019 at the same sites (Athens, Barcelona and Zurich).

2.4.3 eBC

Aethalometer source apportionment analysis was performed between 2020 and 2023 to estimate the contributions of of eBC emitted by combustion of liquid fuel (eBC_{LF}) and solid fuel (eBC_{SF}) at four pilot sites using the Aethalometer model (Sandradewi et al., 2008). This model uses the 7- babs measurements provided by AE instruments and it is based on the fact that solid fuel sources emit eBC together with specific organic aerosols (OA) that can absorb in the UV-VIS spectral range (the so-called Brown Carbon, BrC) thus causing an increase of AAE. The model permit to quantify the contribution of BC emitted by combustion of liquid fuel (eBC_{LF}) and by combustion of solid fuel (eBC_{SF}) mainly from residential and commercial wood and coal burning. The results of the Aethalometer source apportionment model depend on the chosen Absorption Angstrom Exponent (AAE). Usually, two pairs of values are used: 1 and 2 for AAE_{LF} and AAE_{SF}, respectively (Sandradewi et al., 2008), and 0.90 and 1.68, respectively (Zotter et al., 2017). An alternative method involves using the frequency distribution of AAE to estimate site-specific values (Tobler et al., 2021). Here, we applied AAE values of 1 and 2 for source apportionment at pilot sites. For a detailed description of the eBC source apportionment, the related sensitivity study, and the recommendations, please refer to the RI-URBANS service tool document for eBC source apportionment (https://riurbans.eu/wp-content/uploads/2024/07/ST2_BC.pdf). See ST11 on BC source apportionment from RI-URBANS.

2.4.4 Oxidative potential

There is a deliverable in M40 (D30 (D4.9)) on source apportionment of OP and the results will be reported there, not in this milestone's report. The methodology for source apportionment of OP is also reported in ST11 on OP source apportionment from RI-URBANS

RI-URBANS (www.RIURBANS.eu) is supported by the European Commission under the Horizon 2020 – Research and Innovation Framework Programme, H2020-GD-2020, Grant Agreement number: 101036245

3 Results

All the analysis is completed and the results are shared with the RI-URBANS partners at https://www.healthpilot-riurbans.eu/.

3.1 PM composition

PM10 concentrations were higher in Athens (32 µg m^{-3}), lower in Paris (23 µg m^{-3}) and Barcelona (22 µg m^{-3}), and lowest in Zurich (16 µg m^{-3}). PM2.5 concentrations were substantially lower but otherwise showed a similar spatial behaviour: Athens (24 µg m^{-3}), Barcelona (15 µg m^{-3}), Paris (11 µg m^{-3}), Zurich (11 µg m^{-3}). The PM2.5 and PM10 chemical analyses of trace elements, water-soluble inorganic ions, organic and elemental carbon are used for reconstructing the gravimetrically determined mass concentration (Figure 3). The chemically reconstructed mass accounts for 75% in Barcelona, 86% in Paris, 91% in Athens, and 96% in Zurich. The lowest chemically reconstructed PM mass fraction in Barcelona can be related to higher humidity or to a higher contribution of secondary organic aerosols (SOA; underestimation of OM). In addition, there is a good correlation between PM10 daily concentrations and total mass determined at all sites (Figure 4).

The main PM10 constituents are displayed in Figure 3. In Athens, with a drier climate and a more pronounced desert influence, dust is a larger contributor to PM10 than at the other locations. Secondary inorganic aerosol (SIA, sulphate, nitrate, ammonium) as well as Organic Matter (OM) are other substantial contributors to PM at all locations. We found that the organic carbon is to a substantial amount water-soluble without much variation between the pilot cities (Athens: 38%, Barcelona 43%, Paris 42%, Zurich 43%). Based on the targeted characterizations of organic compounds we observe a strongly enhanced impact of biomass burning tracers in winter, while in summer of oxidation products of biogenic volatile organic compound emissions are clearly enhanced (see example for Barcelona in Figure 5). This is further confirmed based on the non-targeted mass spectral data (see example EESI-MS mass spectra in Figure 6). In summer many high intensity peaks were found in laboratory SOA generated from alpha-pinene. In winter, the dominant impact of $C_6H_{10}O_5$ (likely levoglucosan) showcases the importance of residential biomass burning on WSOA.

RI-URBANS (www.RIURBANS.eu) is supported by the European Commission under the Horizon 2020 – Research and Innovation Framework Programme, H2020-GD-2020, Grant Agreement number: 101036245

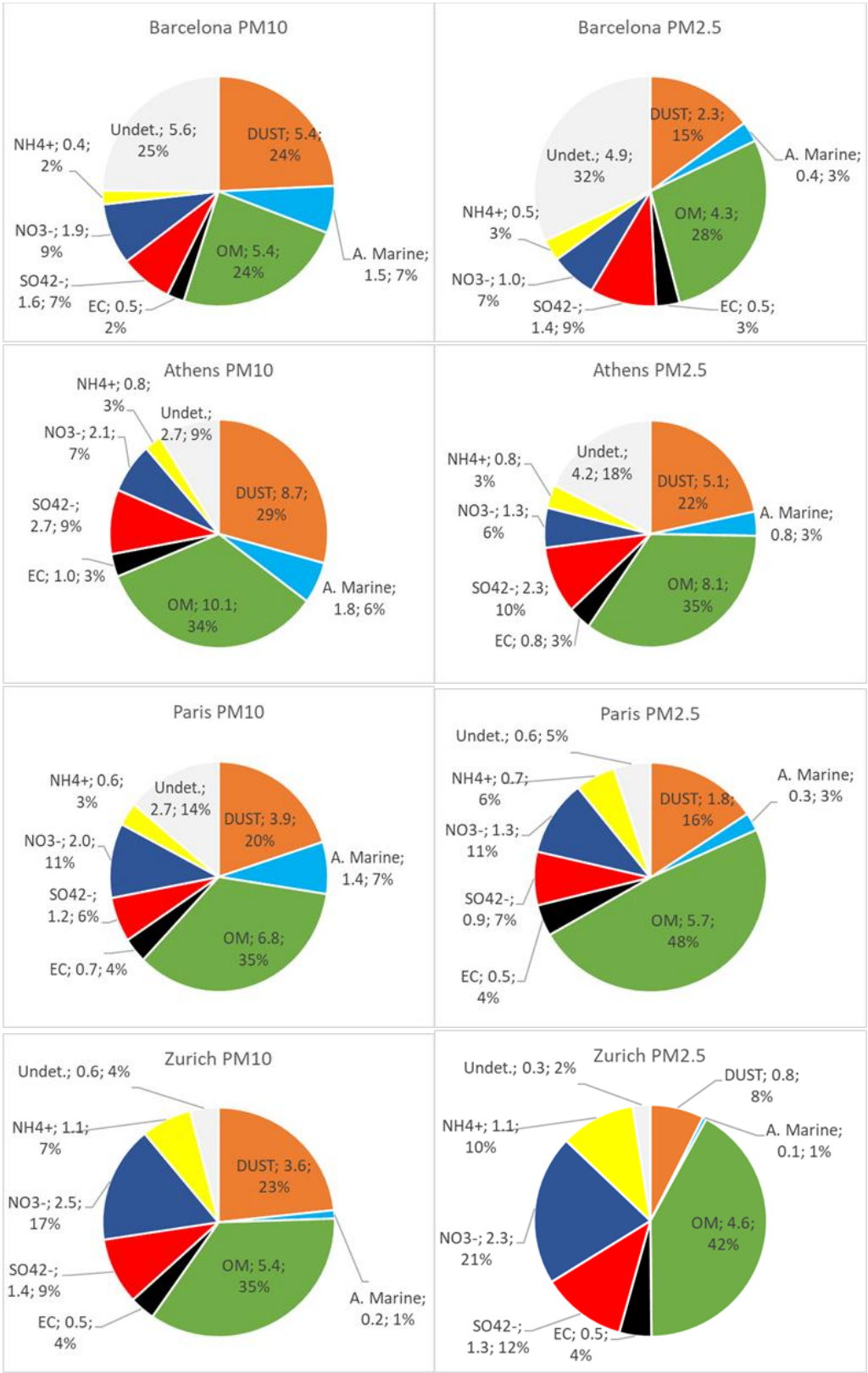

***Figure 3**. Average contribution of major groups of elements (Mineral dust; Marine aerosol; Organic matter, and SIA) for 4 pilot cities for PM_{10} (left column) and $PM_{2.5}$ (right column).*

RI-URBANS (www.RIURBANS.eu) is supported by the European Commission under the Horizon 2020 – Research and Innovation Framework Programme, H2020-GD-2020, Grant Agreement number: 101036245

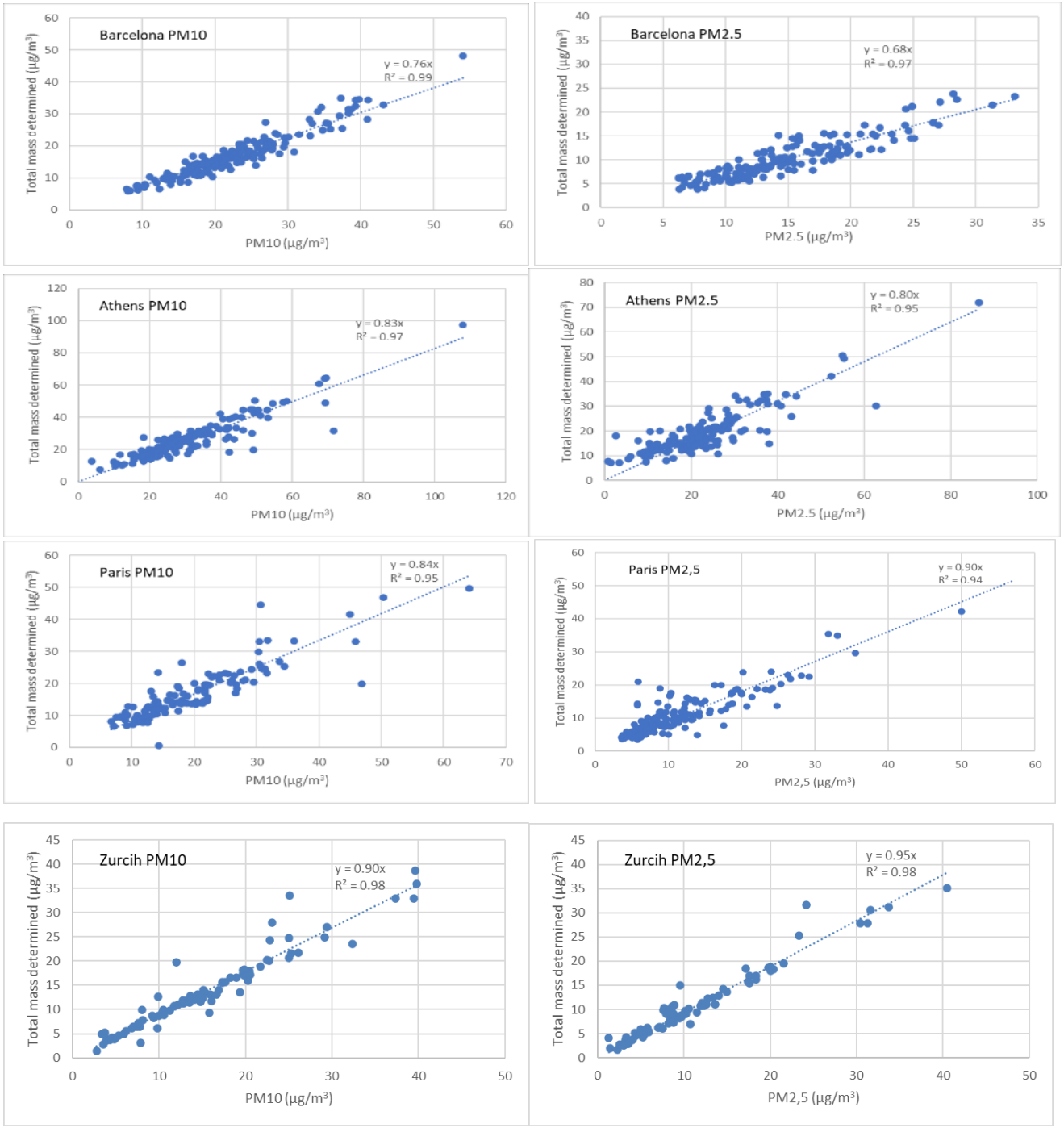

***Figure 4**. Scatter-plots showing correlations between daily PM10 concentrations and total mass determined per each filter (dust+marine aerosol+OM+EC+SIA) for 4 pilot cities for $PM_{2.5}$ (left column) and PM_{10} (right column).*

RI-URBANS (www.RIURBANS.eu) is supported by the European Commission under the Horizon 2020 – Research and Innovation Framework Programme, H2020-GD-2020, Grant Agreement number: 101036245

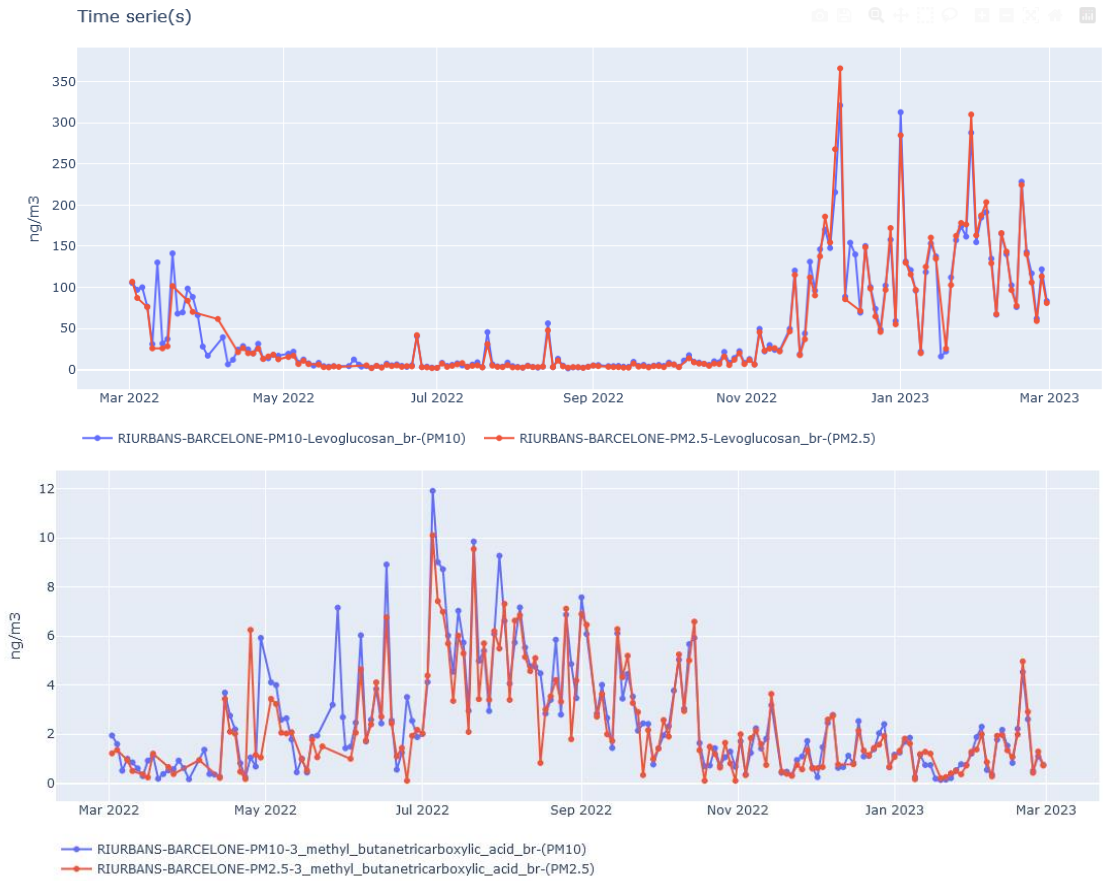

Figure 5. *Concentration time series of levoglucosan (biomass burning POA marker) and MBTCA (an oxidation product of alpha-pinene - a biogenic SOA marker) in Barcelona in PM10 (blue) and PM2.5 (red). The Figure is generated by https://www.healthpilot-riurbans.eu.*

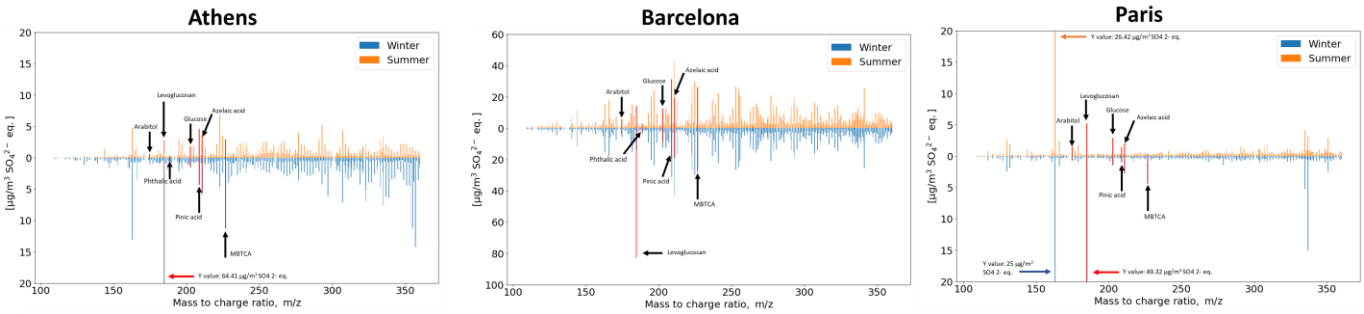

Figure 6*. Near-molecular characterizations of WSOA via Extractive ElectroSpray Ionization Mass spectrometry (EESI-MS) for Barcelona, Athens, Paris separated for summer and winter.*

RI-URBANS (www.RIURBANS.eu) is supported by the European Commission under the Horizon 2020 – Research and Innovation Framework Programme, H2020-GD-2020, Grant Agreement number: 101036245

3.2 Brown carbon

The sites of Athens, Paris and Barcelona presented a yearly average BrC absorption coefficient ($Abs_{WS\_BrC\_365}$) of 2.04, 1.16, 0.88 Mm^{-1}, respectively for fine aerosol (PM2.5); while the corresponding values for PM10 fractions were 2.59, 1.65, 0.99 Mm^{-1}, respectively. The city of Athens reveals the highest water-soluble BrC values, followed by Paris; while the city of Barcelona demonstrates the lowest values on a yearly basis. In the city of Zurich, an absorption coefficient of 0.90 Mm^{-1} was measured for fine aerosol fraction, while the respective water-soluble BrC absorption coefficient for PM10 was estimated at 1.03 Mm^{-1}; the latter values appear to be similar to the levels recorded in the city of Barcelona.

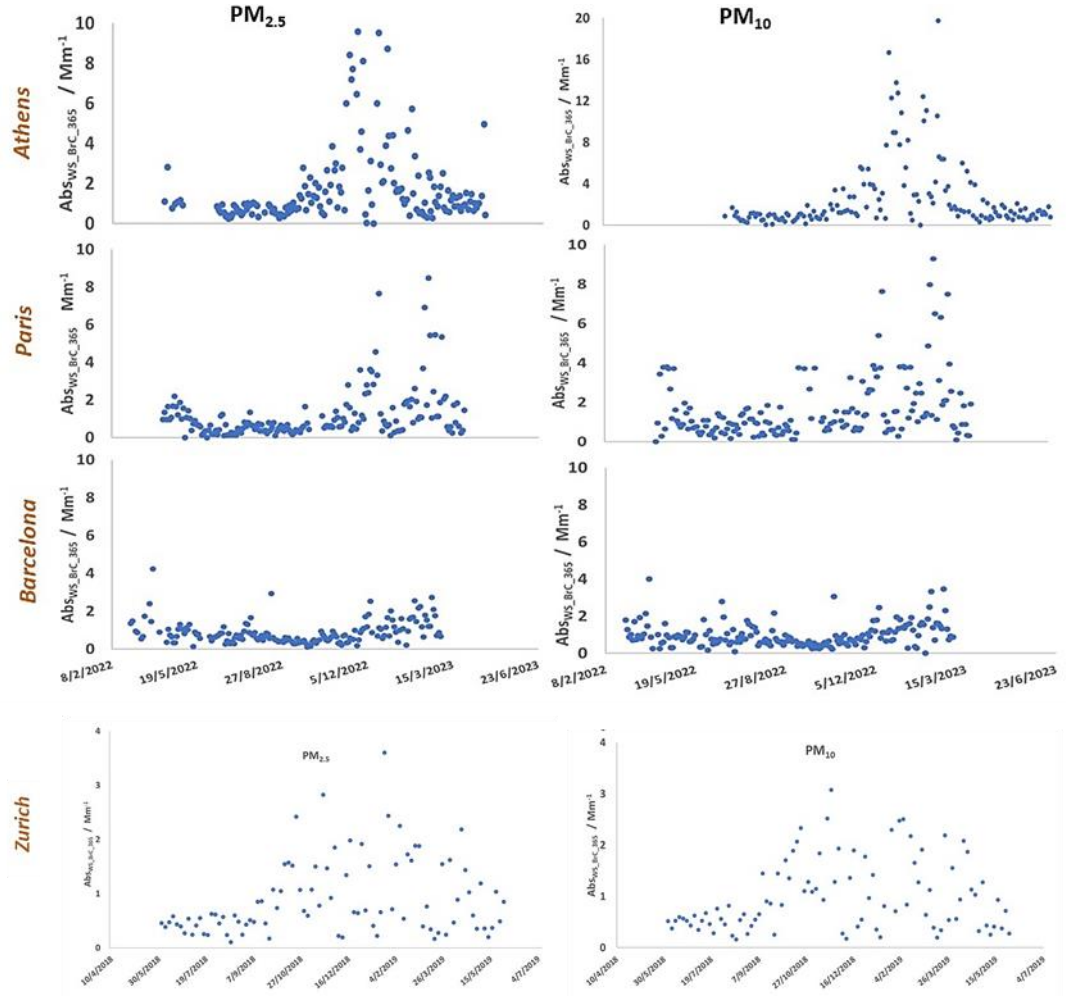

Figure 7. *Time-series (Feb 2022 – Jun 2023) of water-soluble brown carbon (BrC) analyses displayed as BrC absorption coefficient ($Abs_{WS\_BrC\_365}$) for all 4 pilot cities for $PM_{2.5}$ (left column) and PM_{10} (right column).*

RI-URBANS (www.RIURBANS.eu) is supported by the European Commission under the Horizon 2020 – Research and Innovation Framework Programme, H2020-GD-2020, Grant Agreement number: 101036245

3.3 OP

A summary of the OP-DTT analyses is presented in the following for Athens, Barcelona, Paris, and Zurich (Figure 8). The oxidative potential concentration in PM10 is the highest in Athens (2.6 nmol/min/m^3), followed by Paris (1.9 nmol/min/m^3) and Barcelona (1.8 nmol/min/m^3), and the lowest in Zurich (1.3 nmol/min/m^3). While for some pilot cities a strong seasonal variation is apparent (e.g., for Athens), this is not the case for others. On the other hand, in all pilot cities the oxidative potential is substantially higher in PM10 than PM2.5 highlighting the importance of coarse particles.

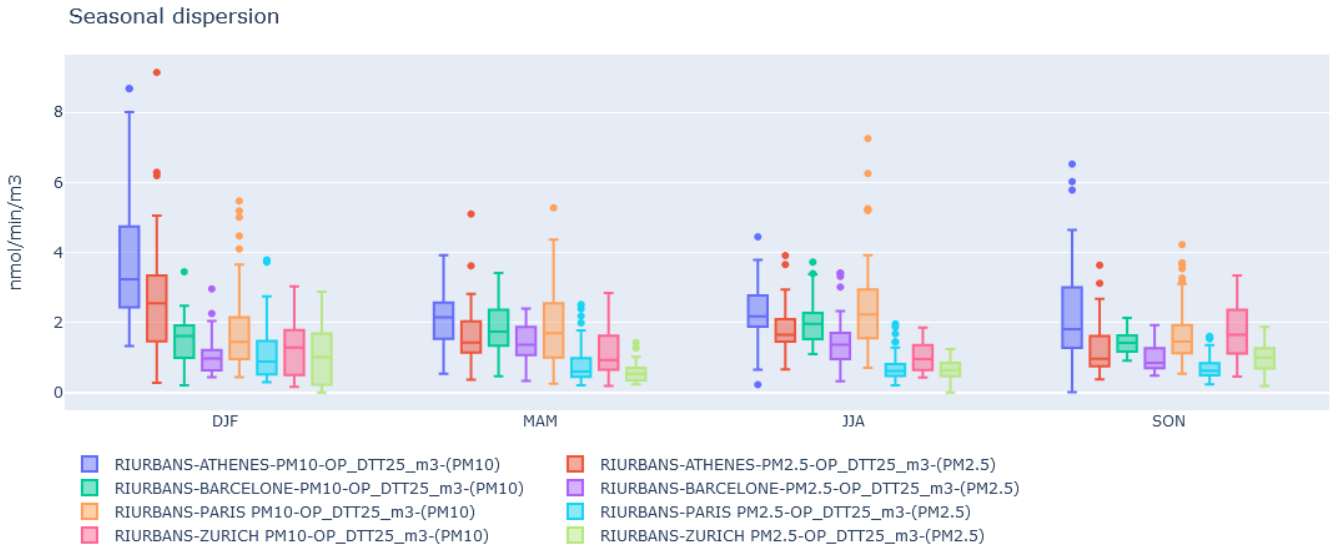

Figure 8. *OP-DTT concentrations (nmol/min/m^3) for the 4 cities separated by size fraction and season (DJF: December-January-February, MAM: March-April-May, JJA: June-July-August, SON: September-October-November): median, 1st and 3rd quantile as well as the upper and lower fence. This Figure is generated by https://www.healthpilot-riurbans.eu.*

RI-URBANS (www.RIURBANS.eu) is supported by the European Commission under the Horizon 2020 – Research and Innovation Framework Programme, H2020-GD-2020, Grant Agreement number: 101036245

3.4 Preliminary results of source apportionment based on PM chemistry

A unified source apportionment analysis for particulate matter is ongoing. In order to devise a PMF strategy, we performed a sensitivity assessment using two contrasting environments (Barcelona, Spain vs. Paris, France). In brief, the PMF input includes the PM mass concentration, trace elements, water-soluble ions, elemental carbon and organic carbon, as well as organic marker compounds for primary wood burning PM (levoglucosan), primary biological PM (polyols), and secondary biogenic PM (3-MBTCA). Preliminary results for Barcelona and Paris are displayed in Figure 9 and 10.

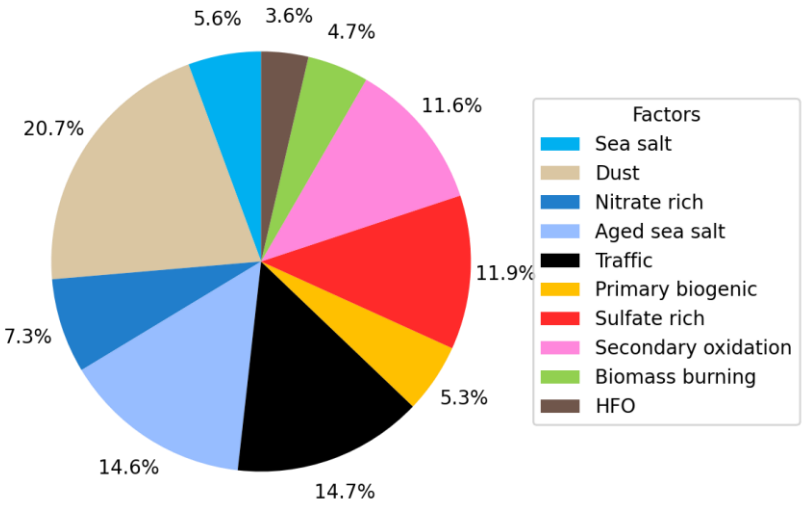

Figure 9. *PM10 sources (or factors) for Barcelona, Spain. Resolved sources are sea salt PM, dust PM, nitrate-rich PM related to secondary PM including secondary organic carbon (SOC), aged sea salt PM, primary traffic PM, primary biogenic PM, sulfate rich PM related to secondary PM including SOC, secondary biogenic PM (secondary oxidation), biomass burning PM, and heavy fuel oil PM (HFO).*

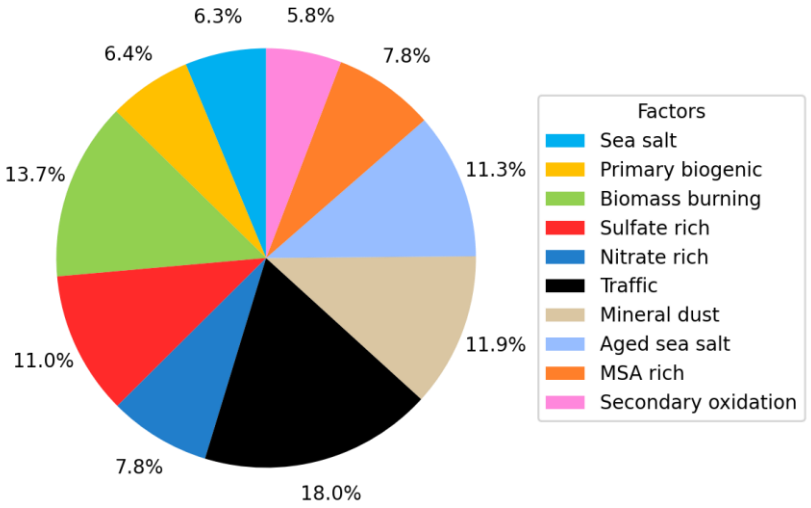

Figure 10. *PM sources (or factors) for Paris, France. Resolved sources are sea salt PM, primary biogenic PM, biomass burning PM, sulfate rich PM related to secondary PM including secondary organic carbon (SOC), nitrate-rich PM related to secondary PM including SOC, primary traffic PM, dust PM, aged sea salt PM, MSA-rich PM, secondary biogenic PM (secondary oxidation).*

RI-URBANS (www.RIURBANS.eu) is supported by the European Commission under the Horizon 2020 – Research and Innovation Framework Programme, H2020-GD-2020, Grant Agreement number: 101036245

3.5 Source apportionment based on eBC data

Data on the eBC mass concentrations as well as the contribution of liquid (eBC_{LF}) and solid fuels (eBC_{SF}) are available at the RI-URBANS shared folder AE33. In this section, we present a summary of the eBC data collected at five pilot sites over the period from 2020 to 2023. eBC concentrations were overall highest in Athens, followed by Barcelona and Paris, and lowest in Zurich. The source contributions, however, do not show the same trend. In line with the more prevalent impact of biomass burning on PM in Athens and Zurich, also eBC is more impacted by eBC_{SF} - from residential biomass burning (Figure 11).

Across all five pilot sites, eBC_{LF} consistently contributes more than eBC_{SF}, with values ranging from 66.5% (ZUR_UB) to 82.5% (PAR_UB). The highest contribution from liquid fuel combustion is observed at PAR_UB (82.5%), followed closely by PAR_TR (80.6%). The contribution of eBC_{SF} varies across the sites but is generally lower than that of eBC_{LF}. The highest relative contribution of eBC_{SF} is observed at ATH_UB (31.6%) and ZUR_UB (33.5%), indicating a more significant presence of solid fuel combustion sources at these sites compared to the others. PAR_UB and PAR_TR show similar dominance of eBC_{LF} with relatively minor contributions from eBC_{SF} (17.5% and 19.4%, respectively). In contrast, locations like ATH_UB and ZUR_UB show a more balanced but still predominant contribution from liquid fuel sources, with solid fuel sources contributing a more substantial portion of eBC. This suggests site-specific differences in the sources of eBC.

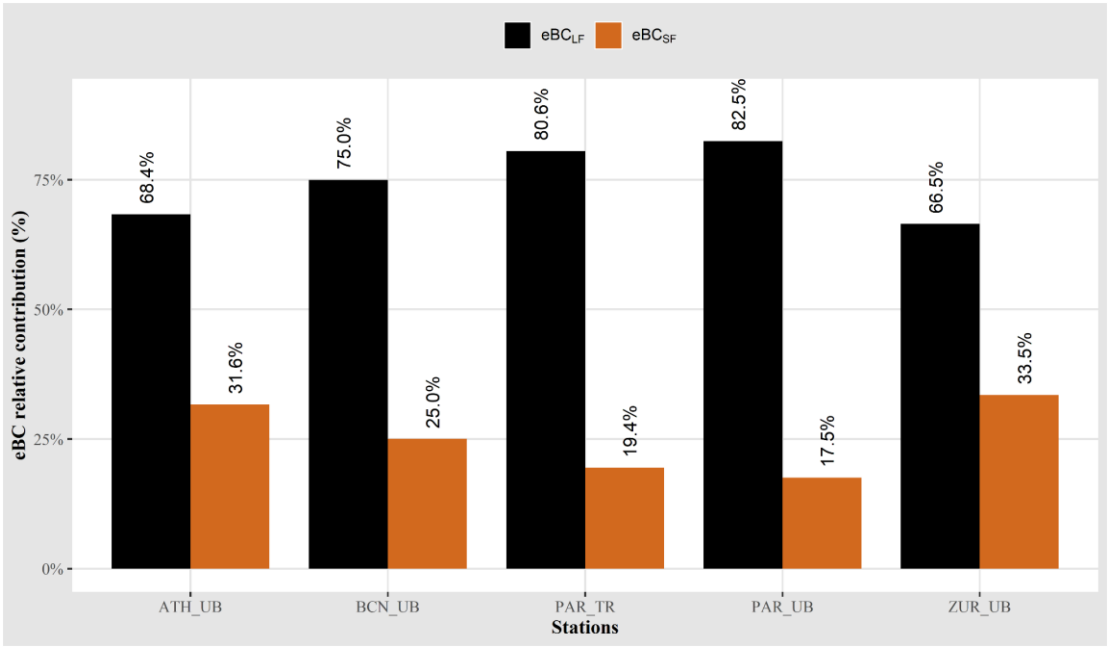

Figure 11. *The relative contributions (%) of eBC from liquid fuel (eBC_{LF}) and solid fuel (eBC_{SF}) at five pilot sites.*

RI-URBANS (www.RIURBANS.eu) is supported by the European Commission under the Horizon 2020 – Research and Innovation Framework Programme, H2020-GD-2020, Grant Agreement number: 101036245

3.6 Source apportionment of UFP-PNSD

From the four pilot cities we report data and source apportionment for two of them (Athens and Barcelona). The pilot measurements yielded results very similar to those from the 2017-2019 data compilation presented in previous reports.

In Barcelona, the average concentrations of PNC were much lower from 2020-2023 (8355 # cm^{-3}) compared to 2017-2019 (11185 # cm^{-3}). However, the percentages of the Nucleation, Aitken, and Accumulation mode size fractions remained similar in both periods (38%, 50%, and 12% from 2017-2019, respectively; and 42%, 46%, and 12% from 2020-2023, respectively). In Athens, average PNC concentrations also decreased, from 8552 # cm^{-3} in 2017-2019 to 6908 # cm^{-3} in 2020-2022. The percentages of the Nucleation, Aitken, and Accumulation mode size fractions were also very similar in both periods (18%, 62%, and 20% from 2017-2019, respectively; and 18%, 60%, and 22% from 2020-2022, respectively).

Figure 12 shows that Barcelona continues to record high UFP in the Nucleation mode fractions, while Athens has higher concentrations in the Aitken mode, as reported in previous reports, probably due to the low NH_3 concentrations in the Athens region (Garcia-Marlès et al., 2024b). Figure 13 shows the marked seasonal pattern of UFP in Athens and the parallelism with that of BC, with the highest concentrations occurring during traffic rush hours and lower values for both PNC and BC in summer. However, Barcelona exhibited a midday PNC peak in addition to rush hours peaks, with no clear seasonal patterns observed for either BC or PNC. Decreasing concentrations of both PNC and BC were recorded during weekends in Barcelona, but this was not seen in Athens. The results from 2020-2023 at both sites were consistent with those from the 2017-2019 period.

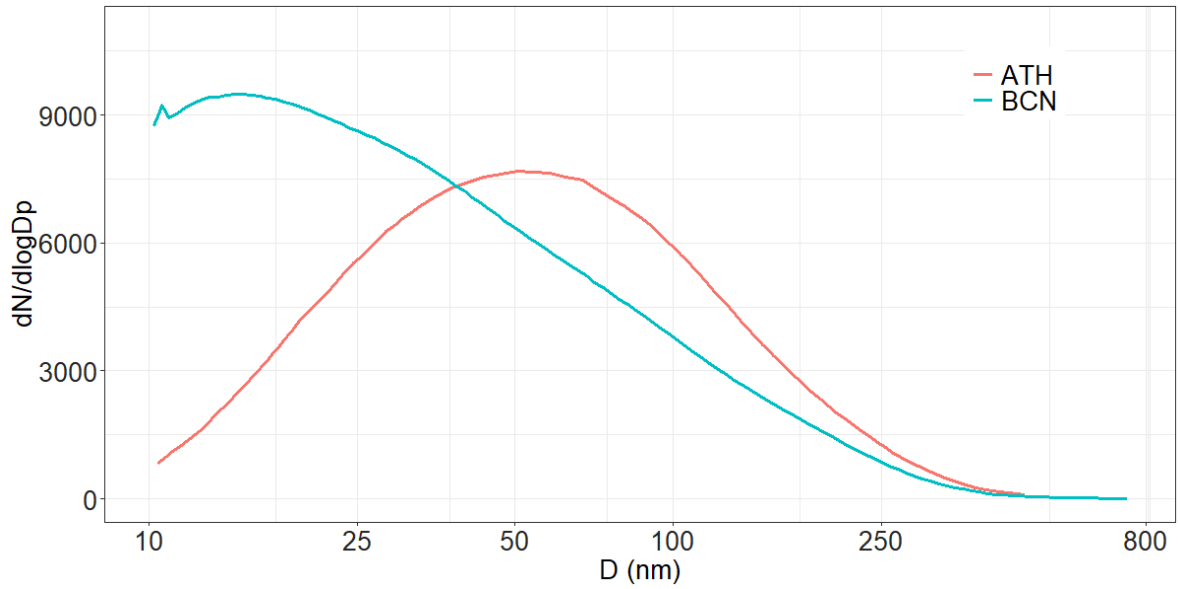

Figure 12. *Averaged Particle Number Size Distributions for Barcelona (BCN) and Athens (ATH) from 2020 to 2023.*

RI-URBANS (www.RIURBANS.eu) is supported by the European Commission under the Horizon 2020 – Research and Innovation Framework Programme, H2020-GD-2020, Grant Agreement number: 101036245

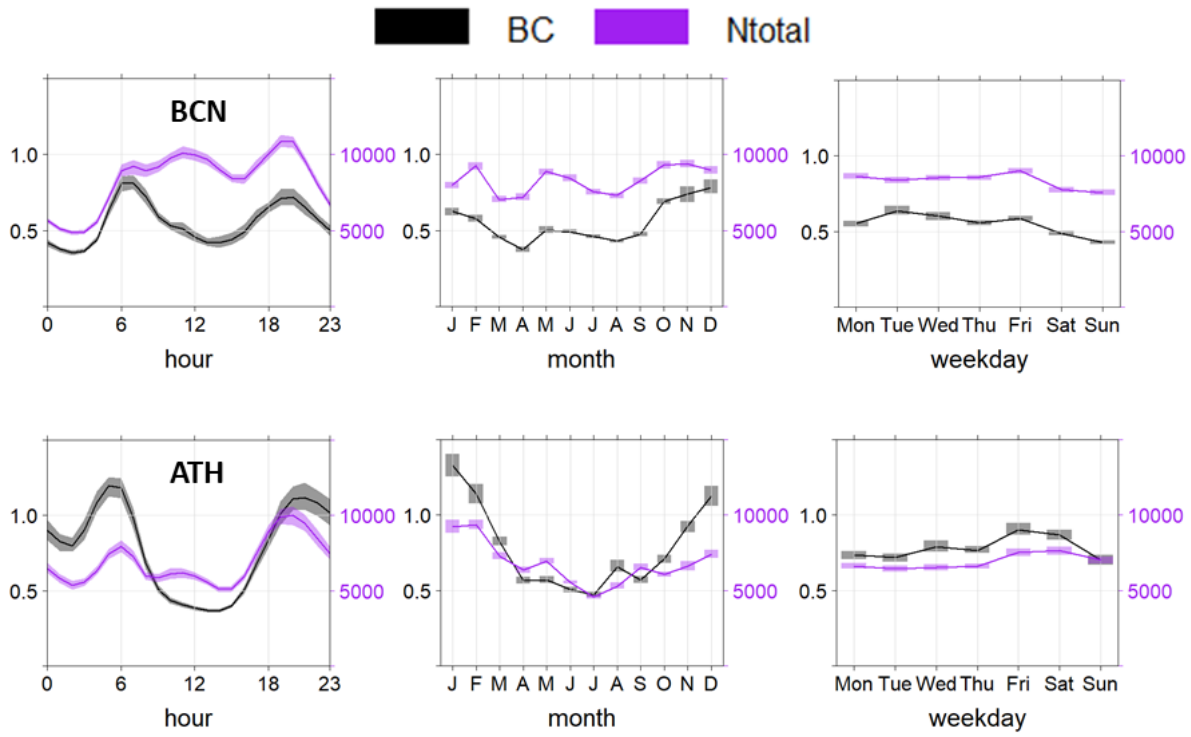

Figure 13. *Averaged hourly concentrations of Particle Number Concentration (Ntotal) and Black Carbon (BC) for Barcelona (BCN) and Athens (ATH) from 2020 to 2023. Particle Number Concentration is expressed in # cm^{-3}, and BC in µg m^{-3}.*

Preliminary source apportionment results of UFP-PNSD are also presented in this report, and the following sources were identified:

- Traffic-1: Major size mode around 25-35 nm. Associated to gasoline vehicle emissions, freshly emitted traffic particles or nucleation of diesel particles. Peaks observed during traffic rush-hours and minimum values occur on weekends.
- Traffic-2: Major size mode around 60-100 nm. Associated to diesel vehicle emissions or coagulation of traffic particles when moving from the sources. Similar patterns to Traffic-1.
- Mixed traffic: Major size mode between those of Traffic 1 & Traffic 2, due to a mix of all traffic sources.
- Photonucleation: Major size mode around 10-20 nm. A midday peak is found when high photochemical activity leads to new particle formation events.
- Urban background: Major size mode around 100-180 nm. It is influenced by traffic emissions, exhibiting similar trends to those of the traffic sources.
- Regional background: Typically showing a bimodal distribution with a primary size mode above 150 nm. Regional-1 reaches its maximum during winter, while in Regional-2 the maximum occurs during summer and at midday.
- Domestic heating: Major size mode around 100 nm. It is associated with the combustion of fuels, and peaks during the night and winter.

Figure 14 shows the relative contributions of PNC from the identified sources in Barcelona and Athens. In Barcelona, traffic (the sum of all traffic sources) contributed 65% of the total PNC during 2020-2023, compared to 61% during 2013-2019. Photonucleation contributed 31% in 2013-2019 and 28% in 2020-2023. In Athens, total traffic contributed 76% during both the 2015-2019 and 2020-2022 periods (including significant contributions from

RI-URBANS (www.RIURBANS.eu) is supported by the European Commission under the Horizon 2020 – Research and Innovation Framework Programme, H2020-GD-2020, Grant Agreement number: 101036245

Domestic heating, which could not be separated from Traffic-2). Photonucleation contributions slightly decreased, from 14% during 2015-2019 to 11% during 2020-2022, and domestic heating keeps a high contribution to UFP in this city.

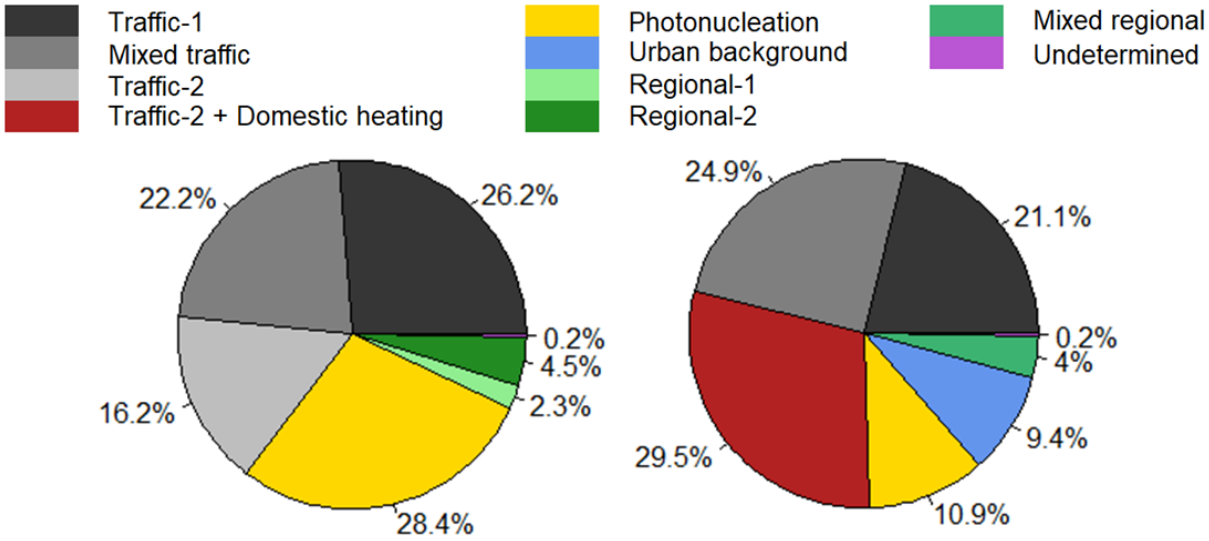

Figure 14. *Relative contributions (%) of Particle Number Concentration (PNC) from the identified sources at Barcelona (BCN, left and Athens (ATH, right) from 2020 to 2023. The Undetermined category (in purple) represents the fraction of PNC not assigned to a specific source by PMF.*

4 Further work

Tools for measuring ambient concentrations of PM components, eBC, UFP-PNSD and OP of PM, and for the source apportionment have been produced by RI-URBANS and tested in four pilot cities. These can already be implemented in supersites for the new European AQ Directive. These are described in:

ST10 on PM source apportionment from RI-URBANS

ST11 on BC, UFP, OP and VOCs source apportionment from RI-URBANS

Forthcoming work will focus on i) improvement of the NRT-PM speciation source apportionment, and ii) evaluation of the source apportionment of OP of PM.

Furthermore, the epidemiological evaluation of these and their source contributions is ongoing and will be presented in a WP4 deliverable.

RI-URBANS (www.RIURBANS.eu) is supported by the European Commission under the Horizon 2020 – Research and Innovation Framework Programme, H2020-GD-2020, Grant Agreement number: 101036245

5 References

ACTRIS: Preliminary ACTRIS recommendation for aerosol in-situ sampling, measurements, and analysis. https://www.actris.eu/sites/default/files/2021-06/Preliminary%20ACTRIS%20recommendations%20for%20aerosol%20in-situ%20measurements%20June%202021.pdf, 2021.

Alastuey, A., Querol, X., Aas, W., Lucarelli, F., Pérez, N., Moreno, T., Cavalli, F., Areskoug, H., Balan, V., Catrambone, M., Ceburnis, D., Cerro, J. C., Conil, S., Gevorgyan, L., Hueglin, C., Imre, K., Jaffrezo, J. L., Leeson, S. R., Mihalopoulos, N., Mitosinkova, M., O'Dowd, C. D., Pey, J., Putaud, J. P., Riffault, V., Ripoll, A., Sciare, J., Sellegri, K., Spindler, G., and Yttri, K. E.: Geochemistry of PM10 over Europe during the EMEP intensive measurement periods in summer 2012 and winter 2013, Atmos. Chem. Phys., 16, 6107-6129, 10.5194/acp-16-6107-2016, 2016.

Alier, M., van Drooge, B. L., Dall'Osto, M., Querol, X., Grimalt, J. O., and Tauler, R.: Source apportionment of submicron organic aerosol at an urban background and a road site in Barcelona (Spain) during SAPUSS, Atmos. Chem. Phys., 13, 10353-10371, 10.5194/acp-13-10353-2013, 2013.

Amato, F., Pandolfi, M., Escrig, A., Querol, X., Alastuey, A., Pey, J., Perez, N., and Hopke, P. K.: Quantifying road dust resuspension in urban environment by Multilinear Engine: A comparison with PMF2, Atmospheric Environment, 43, 2770-2780, https://doi.org/10.1016/j.atmosenv.2009.02.039, 2009.

Atwi, K., Cheng, Z., El Hajj, O., Perrie, C., and Saleh, R.: A dominant contribution to light absorption by methanol-insoluble brown carbon produced in the combustion of biomass fuels typically consumed in wildland fires in the United States, Environmental Science: Atmospheres, 2, 182-191, 10.1039/D1EA00065A, 2022.

Belis, C. A., Favez, O., Mircea, M., Diapouli, E., Manousakas, M. I., Vratolis, S., Gilardoni, S., Paglione, M., Decesari, S., Mocnik, G., Mooibroek, D., Salvador, P., Takahama, S., Vecchi, R., and Paatero, P.: European guide on air pollution source apportionment with receptor models - Revised version 2019. EUR 29816 EN. , Joint Research Centre (European Commission). JRC117306. Publications Office of the European Union, Luxembourg, 2019. https://data.europa.eu/doi/10.2760/439106, 2019.

Borlaza, L. J. S., Weber, S., Uzu, G., Jacob, V., Cañete, T., Micallef, S., Trébuchon, C., Slama, R., Favez, O., and Jaffrezo, J. L.: Disparities in particulate matter (PM10) origins and oxidative potential at a city scale (Grenoble, France) – Part 1: Source apportionment at three neighbouring sites, Atmos. Chem. Phys., 21, 5415-5437, 10.5194/acp-21-5415-2021, 2021.

Brown, R. J., Beccaceci, S., Butterfield, D. M., Quincey, P. G., Harris, P. M., Maggos, T., Panteliadis, P., John, A., Jedynska, A., and Kuhlbusch, T. A.: Standardisation of a European measurement method for organic carbon and elemental carbon in ambient air: results of the field trial campaign and the determination of a measurement uncertainty and working range, Environmental Science: Processes & Impacts, 19, 1249-1259, 2017.

Calas, A., Uzu, G., Martins, J. M. F., Voisin, D., Spadini, L., Lacroix, T., and Jaffrezo, J.-L.: The importance of simulated lung fluid (SLF) extractions for a more relevant evaluation of the oxidative potential of particulate matter, Scientific Reports, 7, 11617, 10.1038/s41598-017-11979-3, 2017.

Calas, A., Uzu, G., Kelly, F. J., Houdier, S., Martins, J. M., Thomas, F., Molton, F., Charron, A., Dunster, C., and Oliete, A.: Comparison between five acellular oxidative potential measurement assays performed with detailed chemistry on PM 10 samples from the city of Chamonix (France), Atmos. Chem. Phys., 18, 7863-7875, 2018.

RI-URBANS (www.RIURBANS.eu) is supported by the European Commission under the Horizon 2020 – Research and Innovation Framework Programme, H2020-GD-2020, Grant Agreement number: 101036245

Calas, A., Uzu, G., Besombes, J.-L., Martins, J. M. F., Redaelli, M., Weber, S., Charron, A., Albinet, A., Chevrier, F., Brulfert, G., Mesbah, B., Favez, O., and Jaffrezo, J.-L.: Seasonal Variations and Chemical Predictors of Oxidative Potential (OP) of Particulate Matter (PM), for Seven Urban French Sites, Atmosphere, 10, 698, 2019.

Carslaw, D. C. and Ropkins, K.: openair — An R package for air quality data analysis, Environmental Modelling & Software, 27-28, 52-61, https://doi.org/10.1016/j.envsoft.2011.09.008, 2012.

Cavalli, F., Viana, M., Yttri, K. E., Genberg, J., and Putaud, J. P.: Toward a standardised thermal-optical protocol for measuring atmospheric organic and elemental carbon: the EUSAAR protocol, Atmos. Meas. Tech., 3, 79-89, 10.5194/amt-3-79-2010, 2010.

CEN/–S16976:2016: CEN Standard for Ambient air - Determination of the particle number concentration of atmospheric aerosol. https://standards.iteh.ai/catalog/standards/cen/91f1ac67-f6d6-408c-af89-e81763194fd3/cen-ts-16976-2016.

CEN/TS17434:2020: Standard for Ambient air - Determination of the particle number size distribution of atmospheric aerosol using a Mobility Particle Size Spectrometer (MPSS). https://standards.iteh.ai/catalog/standards/cen/a841bc08-ed34-4fa8-94ca-8c5e07b99db9/cen-ts-17434-2020.

CEU, 2024. Proposal for a Directive of the European Parliament and of the Council on ambient air quality and cleaner air for Europe (recast) 08/03/2024. Council of European Union, https://data.consilium.europa.eu/doc/document/ST-7335-2024-INIT/en/pdf

Cui, T., Manousakas, M. I., Wang, Q., Uzu, G., Hao, Y., Khare, P., Qi, L., Chen, Y., Han, Y., Slowik, J. G., Jaffrezo, J.-L., Cao, J., Prévôt, A. S. H., and Daellenbach, K. R.: Composition and Sources of Organic Aerosol in Two Megacities in Western China Using Complementary Mass Spectrometric and Statistical Techniques, ACS ES&T Air, 10.1021/acsestair.4c00051, 2024.

Daellenbach, K. R., Uzu, G., Jiang, J., Cassagnes, L.-E., Leni, Z., Vlachou, A., Stefenelli, G., Canonaco, F., Weber, S., and Segers, A.: Sources of particulate-matter air pollution and its oxidative potential in Europe, Nature, 587, 414-419, https://doi.org/10.1038/s41586-020-2902-8, 2020.

Daellenbach, K. R., Bozzetti, C., Křepelová, A., Canonaco, F., Wolf, R., Zotter, P., Fermo, P., Crippa, M., Slowik, J. G., Sosedova, Y., Zhang, Y., Huang, R. J., Poulain, L., Szidat, S., Baltensperger, U., El Haddad, I., and Prévôt, A. S. H.: Characterization and source apportionment of organic aerosol using offline aerosol mass spectrometry, Atmos. Meas. Tech., 9, 23-39, https://doi.org/10.5194/amt-9-23-2016, 2016.

Drinovec, L., Močnik, G., Zotter, P., Prévôt, A. S. H., Ruckstuhl, C., Coz, E., Rupakheti, M., Sciare, J., Müller, T., Wiedensohler, A., and Hansen, A. D. A.: The "dual-spot" Aethalometer: an improved measurement of aerosol black carbon with real-time loading compensation, Atmos. Meas. Tech., 8, 1965-1979, 10.5194/amt-8-1965-2015, 2015.

EN12341:2014: European Committee for Standardization (CEN). Ambient air - Standard gravimetric measurement method for the determination of the PM10 or PM2,5 mass concentration of suspended particulate matter. .

EN14907:2005: Ambient air quality - Standard gravimetric measurement method for the determination of the PM2,5 mass fraction of suspended particulate matter.

EN16909:2017: European Committee for Standardisation (CEN). Ambient Air Measurement of Elemental Carbon (EC) and Organic Carbon (OC) Collected on Filters.

RI-URBANS (www.RIURBANS.eu) is supported by the European Commission under the Horizon 2020 – Research and Innovation Framework Programme, H2020-GD-2020, Grant Agreement number: 101036245

EN16913:2017: 'Ambient air - Standard method for measurement of NO3-, SO42-, Cl-, NH4+, Na+, K+, Mg2+, Ca2+ in PM2.5 as deposited on filters'.

Fontal, M., van Drooge, B. L., López, J. F., Fernández, P., and Grimalt, J. O.: Broad spectrum analysis of polar and apolar organic compounds in submicron atmospheric particles, Journal of Chromatography A, 1404, 28-38, https://doi.org/10.1016/j.chroma.2015.05.042, 2015.

Garcia-Marlès, M., Lara, R., Reche, C., Pérez, N., Tobías, A., Savadkoohi, M., Beddows, D., Salma, I., Vörösmarty, M., Weidinger, T., Hueglin, C., Mihalopoulos, N., Grivas, G., Kalkavouras, P., Ondráček, J., Zíková, N., Niemi, J. V., Manninen, H. E., Green, D. C., Tremper, A. H., Norman, M., Vratolis, S., Eleftheriadis, K., Gómez-Moreno, F. J., Alonso-Blanco, E., Wiedensohler, A., Weinhold, K., Merkel, M., Bastian, S., Hoffmann, B., Altug, H., Petit, J.-E., Favez, O., Dos Santos, S. M., Putaud, J.-P., Dinoi, A., Contini, D., Timonen, H., Lampilahti, J., Petäjä, T., Pandolfi, M., Hopke, P. K., Harrison, R. M., Alastuey, A., and Querol, X.: Inter-annual trends of ultrafine particles in urban Europe, Environment International, 185, 108510, https://doi.org/10.1016/j.envint.2024.108510, 2024a.

Garcia-Marlès, M., Lara, R., Reche, C., Pérez, N., Tobías, A., Savadkoohi, M., and Querol, X.: Source apportionment of ultrafine particles in urban Europe, Environ. Int. (Submitted), 2024b.

Gianini, M. F. D., Piot, C., Herich, H., Besombes, J. L., Jaffrezo, J. L., and Hueglin, C.: Source apportionment of PM10, organic carbon and elemental carbon at Swiss sites: An intercomparison of different approaches, Science of The Total Environment, 454-455, 99-108, https://doi.org/10.1016/j.scitotenv.2013.02.043, 2013.

Glojek, K., Dinh Ngoc Thuy, V., Weber, S., Uzu, G., Manousakas, M., Elazzouzi, R., Džepina, K., Darfeuil, S., Ginot, P., Jaffrezo, J. L., Žabkar, R., Turšič, J., Podkoritnik, A., and Močnik, G.: Annual variation of source contributions to PM10 and oxidative potential in a mountainous area with traffic, biomass burning, cement-plant and biogenic influences, Environment International, 189, 108787, https://doi.org/10.1016/j.envint.2024.108787, 2024.

Hecobian, A., Zhang, X., Zheng, M., Frank, N., Edgerton, E. S., and Weber, R. J.: Water-Soluble Organic Aerosol material and the light-absorption characteristics of aqueous extracts measured over the Southeastern United States, Atmos. Chem. Phys., 10, 5965-5977, 10.5194/acp-10-5965-2010, 2010.

Hopke, P. K., Chen, Y., Rich, D. Q., Mooibroek, D., and Sofowote, U. M.: The application of positive matrix factorization with diagnostics to BIG DATA, Chemometrics and Intelligent Laboratory Systems, 240, 104885, https://doi.org/10.1016/j.chemolab.2023.104885, 2023.

Karanasiou, A., Minguillón, M. C., Viana, M., Alastuey, A., Putaud, J. P., Maenhaut, W., Panteliadis, P., Močnik, G., Favez, O., and Kuhlbusch, T. A. J.: Thermal-optical analysis for the measurement of elemental carbon (EC) and organic carbon (OC) in ambient air a literature review, Atmos. Meas. Tech. Discuss., 2015, 9649-9712, 10.5194/amtd-8-9649-2015, 2015.

Mircea, M., Calori, G., Pirovano, G., and Belis, C.: European guide on air pollution source apportionment for particulate matter with source-oriented models and their combined use with receptor models. , EUR 30082 EN, Publications Office of the European Union, Luxembourg. , 10.2760/470628, JRC119067, 2020.

Moreno, T., Querol, X., Alastuey, A., Viana, M., Salvador, P., Sánchez de la Campa, A., Artiñano, B., de la Rosa, J., and Gibbons, W.: Variations in atmospheric PM trace metal content in Spanish towns: Illustrating the chemical complexity of the inorganic urban aerosol cocktail, Atmospheric Environment, 40, 6791-6803, https://doi.org/10.1016/j.atmosenv.2006.05.074, 2006.

Norris, G., Duvall, R., Brown, S., and Bai, S.: EPA Positive Matrix Factorization (PMF) 5.0 Fundamentals and User Guide, 2014.

RI-URBANS (www.RIURBANS.eu) is supported by the European Commission under the Horizon 2020 – Research and Innovation Framework Programme, H2020-GD-2020, Grant Agreement number: 101036245

Nozaki, Y.: A fresh look at element distribution in the North Pacific Ocean, Eos, Transactions American Geophysical Union, 78, 221-221, https://doi.org/10.1029/97EO00148, 1997.

Paatero, P.: The multilinear engine—a table-driven, least squares program for solving multilinear problems, including the n-way parallel factor analysis model, J. Comput. Graph. Stat., 8, 854-888, https://doi.org/10.1080/10618600.1999.10474853, 1999.

Paatero, P. and Tapper, U.: Positive matrix factorization: A non-negative factor model with optimal utilization of error estimates of data values, Environmentrics, 5, 111-126, https://doi.org/10.1002/env.3170050203, 1994.

Paraskevopoulou, D., Liakakou, E., Gerasopoulos, E., and Mihalopoulos, N.: Sources of atmospheric aerosol from long-term measurements (5years) of chemical composition in Athens, Greece, Science of The Total Environment, 527-528, 165-178, https://doi.org/10.1016/j.scitotenv.2015.04.022, 2015.

Paraskevopoulou, D., Kaskaoutis, D. G., Grivas, G., Bikkina, S., Tsagkaraki, M., Vrettou, I. M., Tavernaraki, K., Papoutsidaki, K., Stavroulas, I., Liakakou, E., Bougiatioti, A., Oikonomou, K., Gerasopoulos, E., and Mihalopoulos, N.: Brown carbon absorption and radiative effects under intense residential wood burning conditions in Southeastern Europe: New insights into the abundance and absorptivity of methanol-soluble organic aerosols, Science of The Total Environment, 860, 160434, https://doi.org/10.1016/j.scitotenv.2022.160434, 2023.

Querol, X., Alastuey, A., Rodriguez, S., Plana, F., Ruiz, C. R., Cots, N., Massagué, G., and Puig, O.: PM10 and PM2.5 source apportionment in the Barcelona Metropolitan area, Catalonia, Spain, Atmospheric Environment, 35, 6407-6419, https://doi.org/10.1016/S1352-2310(01)00361-2, 2001.

Sandradewi, J., Prévôt, A. S. H., Szidat, S., Perron, N., Alfarra, M. R., Lanz, V. A., Weingartner, E., and Baltensperger, U.: Using Aerosol Light Absorption Measurements for the Quantitative Determination of Wood Burning and Traffic Emission Contributions to Particulate Matter, Environmental Science & Technology, 42, 3316-3323, 10.1021/es702253m, 2008.

Savadkoohi, M., Pandolfi, M., Reche, C., Niemi, J. V., Mooibroek, D., Titos, G., Green, D. C., Tremper, A. H., Hueglin, C., Liakakou, E., Mihalopoulos, N., Stavroulas, I., Artiñano, B., Coz, E., Alados-Arboledas, L., Beddows, D., Riffault, V., De Brito, J. F., Bastian, S., Baudic, A., Colombi, C., Costabile, F., Chazeau, B., Marchand, N., Gómez-Amo, J. L., Estellés, V., Matos, V., van der Gaag, E., Gille, G., Luoma, K., Manninen, H. E., Norman, M., Silvergren, S., Petit, J.-E., Putaud, J.-P., Rattigan, O. V., Timonen, H., Tuch, T., Merkel, M., Weinhold, K., Vratolis, S., Vasilescu, J., Favez, O., Harrison, R. M., Laj, P., Wiedensohler, A., Hopke, P. K., Petäjä, T., Alastuey, A., and Querol, X.: The variability of mass concentrations and source apportionment analysis of equivalent black carbon across urban Europe, Environment International, 178, 108081, https://doi.org/10.1016/j.envint.2023.108081, 2023.

Shetty, N. J., Pandey, A., Baker, S., Hao, W. M., and Chakrabarty, R. K.: Measuring light absorption by freshly emitted organic aerosols: optical artifacts in traditional solvent-extraction-based methods, Atmos. Chem. Phys., 19, 8817-8830, 10.5194/acp-19-8817-2019, 2019.

Srinivas, B., Rastogi, N., Sarin, M. M., Singh, A., and Singh, D.: Mass absorption efficiency of light absorbing organic aerosols from source region of paddy-residue burning emissions in the Indo-Gangetic Plain, Atmospheric Environment, 125, 360-370, https://doi.org/10.1016/j.atmosenv.2015.07.017, 2016.

Theodosi, C., Tsagkaraki, M., Zarmpas, P., Grivas, G., Liakakou, E., Paraskevopoulou, D., Lianou, M., Gerasopoulos, E., and Mihalopoulos, N.: Multi-year chemical composition of the fine-aerosol fraction in Athens, Greece, with emphasis on the contribution of residential heating in wintertime, Atmos. Chem. Phys., 18, 14371-14391, 10.5194/acp-18-14371-2018, 2018.

RI-URBANS (www.RIURBANS.eu) is supported by the European Commission under the Horizon 2020 – Research and Innovation Framework Programme, H2020-GD-2020, Grant Agreement number: 101036245

Tobler, A. K., Skiba, A., Canonaco, F., Močnik, G., Rai, P., Chen, G., Bartyzel, J., Zimnoch, M., Styszko, K., Nęcki, J., Furger, M., Różański, K., Baltensperger, U., Slowik, J. G., and Prevot, A. S. H.: Characterization of non-refractory (NR) PM1 and source apportionment of organic aerosol in Kraków, Poland, Atmos. Chem. Phys., 21, 14893-14906, 10.5194/acp-21-14893-2021, 2021.

Trechera, P., Garcia-Marlès, M., Liu, X., Reche, C., Pérez, N., Savadkoohi, M., Beddows, D., Salma, I., Vörösmarty, M., Casans, A., Casquero-Vera, J. A., Hueglin, C., Marchand, N., Chazeau, B., Gille, G., Kalkavouras, P., Mihalopoulos, N., Ondracek, J., Zikova, N., Niemi, J. V., Manninen, H. E., Green, D. C., Tremper, A. H., Norman, M., Vratolis, S., Eleftheriadis, K., Gómez-Moreno, F. J., Alonso-Blanco, E., Gerwig, H., Wiedensohler, A., Weinhold, K., Merkel, M., Bastian, S., Petit, J.-E., Favez, O., Crumeyrolle, S., Ferlay, N., Martins Dos Santos, S., Putaud, J.-P., Timonen, H., Lampilahti, J., Asbach, C., Wolf, C., Kaminski, H., Altug, H., Hoffmann, B., Rich, D. Q., Pandolfi, M., Harrison, R. M., Hopke, P. K., Petäjä, T., Alastuey, A., and Querol, X.: Phenomenology of ultrafine particle concentrations and size distribution across urban Europe, Environment International, 172, 107744, https://doi.org/10.1016/j.envint.2023.107744, 2023.

van Drooge, B. L., Prats, R. M., Jaén, C., and Grimalt, J. O.: Determination of subpicogram levels of airborne polycyclic aromatic hydrocarbons for personal exposure monitoring assessment, Environmental Monitoring and Assessment, 195, 368, 10.1007/s10661-023-10953-z, 2023.

Waked, A., Favez, O., Alleman, L., Piot, C., Petit, J.-E., Delaunay, T., Verlinden, E., Golly, B., Besombes, J.-L., and Jaffrezo, J.-L.: Source apportionment of PM10 in a north-western Europe regional urban background site (Lens, France) using positive matrix factorization and including primary biogenic emissions, Atmos. Chem. Phys., 14, 3325-3346, 2014.

Weber, S., Salameh, D., Albinet, A., Alleman, L. Y., Waked, A., Besombes, J.-L., Jacob, V., Guillaud, G., Meshbah, B., Rocq, B., Hulin, A., Dominik-Sègue, M., Chrétien, E., Jaffrezo, J.-L., and Favez, O.: Comparison of PM10 Sources Profiles at 15 French Sites Using a Harmonized Constrained Positive Matrix Factorization Approach, Atmosphere, 10, 310, 2019.

Zotter, P., Herich, H., Gysel, M., El-Haddad, I., Zhang, Y., Močnik, G., Hüglin, C., Baltensperger, U., Szidat, S., and Prévôt, A. S. H.: Evaluation of the absorption Ångström exponents for traffic and wood burning in the Aethalometer-based source apportionment using radiocarbon measurements of ambient aerosol, Atmos. Chem. Phys., 17, 4229-4249, 10.5194/acp-17-4229-2017, 2017.

RI-URBANS (www.RIURBANS.eu) is supported by the European Commission under the Horizon 2020 – Research and Innovation Framework Programme, H2020-GD-2020, Grant Agreement number: 101036245